Influence of Interface Roughness on the Fatigue Life of Thermal Barrier Coatings

Robert Eriksson[1,*], Sören Sjöström[1], Håkan Brodin[1,2], Sten Johansson[1], Lars Östergren[3], Xin-Hai Li[2]

[1] Department of Management and Engineering, Linköping University, Linköping SE-58183, Sweden
[2] Siemens Industrial Turbomachinery AB, Finspong SE- 61283, Sweden
[3]GKN Aerospace Engine Systems, Trollhättan SE-46181, Sweden
* Corresponding author: robert.eriksson@liu.se

Abstract Thermal barrier coatings (TBC) are coating system comprising a heat insulating ceramic coating deposited on top of a oxidation resistant metallic coating. During thermal cycling, cracks grow in the metal/ceramic interface which causes the coating system to fail. In order to model such crack growth by finite element (FE) modelling, accurate interface models must be developed. The presented research studies the influence of interface roughness on the thermal fatigue life of TBCs, and suggests how interface models can be derived from interface roughness parameters. High interface roughness was found to promote longer fatigue lives. Interface models were derived from the roughness parameters Rc, Ra, RSm and Rdq and used for FE modelling of crack growth in the interface. The calculated stress intensities, KI and KII, increased with increasing interface roughness and thereby did not predict a slower crack growth with higher interface roughness as was observed experimentally.

Keywords Thermal barrier coating, Interface, Roughness, Fatigue

1. Introduction

Thermal barrier coating (TBC) systems are coating system containing a heat resistant ceramic top coat (TC), and an oxidation resistant metallic bond coat (BC) [1-4]. Such TBC systems are widely in use in gas turbines to provide heat insulation and oxidation protection for structural parts in the combustor and turbine sections; thereby prolonging the life of structural parts, as well as increasing efficiency by enabling higher combustion temperatures [1-4].

During operation, the TBC system is subjected to thermal fatigue. Thermal loads arise from the difference in coefficient of thermal expansion (CTE) of the ceramic top coat and the metallic bond coat [5-7]. Failure of TBCs often occurs close to the BC/TC interface where fatigue cracks grow under a stress field influenced by: the mismatch in CTE, the BC/TC interface roughness and the growing layer of thermally grown oxides (TGO) that form in the interface [5-7].

Predicting TBC life is a matter of great concern and several approaches to the subject exist; one of which is a fracture mechanical approach involving finite element (FE) modelling of crack growth in the BC/TC interface [5,6]. To perform such FE modelling, the BC/TC interface must be accurately modelled. The sine wave has emerged as a common interface model with amplitudes and wavelengths roughly in the intervals 5–20 μm and 20–150 μm respectively [7-13]. However, an in-depth study of the actual BC/TC interface roughness, and its influence on fatigue life, is still missing. Among the few attempts on the subject, Casu et al. [9] can be mentioned, who performed FE modelling for an interface geometry derived from an actual BC/TC interface.

The current research studies the interface characteristics by the means of common surface roughness parameters, and suggests how these can be used to create interface models. TBC coated specimens with various interface roughness were thermally cycled until failure, cross-sectioned and image analysis was used to obtain the interface roughness. The interface roughness parameters were

then used to create interface models. FE modelling of a crack growing in the interface was performed to test whether interface geometries derived in such a way would capture the experimental results from thermal fatigue testing.

1.1. Roughness parameters

The roughness parameters used in this paper are explained by Fig. 1 and Eq. (1)–(4); for further information about roughness parameters see, for example, Gadelmawla et al. [14]. In summary, it may be said that *Rc* and *Ra* are *amplitude parameters* (i.e. they contain information about profile height), *RSm* is a *spacing parameter* (i.e. contains information about profile spacing) and *RΔq* is a *hybrid parameter* (i.e. contains information about both profile height and spacing).

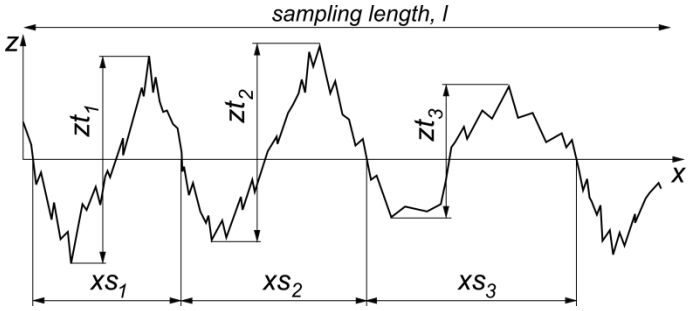

Figure 1. Generic roughness profile.

$$Rc = \frac{1}{n}\sum_{i=1}^{n} zt_i \tag{1}$$

$$Ra = \frac{1}{l}\int_0^l |z(x)|dx \tag{2}$$

$$RSm = \frac{1}{n}\sum_{i=1}^{n} xs_i \tag{3}$$

$$R\Delta q = \sqrt{\frac{1}{l}\int_0^l \left(\frac{dz}{dx}\right)^2 dx} \tag{4}$$

2. Experimental

2.1. Thermal cycling fatigue

Four TBC coated specimens with varyingly coarse BC/TC interfaces were put through thermal cycling until failure. The specimen substrates were cut from 5 mm thick Haynes 230 sheet material in 30x50 mm rectangles. The substrates were coated by 200 µm of NiCrAlY deposited by vacuum plasma spraying, and 350 µm of 7%-yttria partially-stabilised zirconia deposited by atmospheric plasma spraying (APS). The variation in BC/TC roughness was accomplished by using different feedstock powder sizes during spraying of the bond coat.

The specimens were thermally cycled in a furnace until failure. The cycle included heating to 1100 °C for 1 h, and cooling to 100 °C by forced airflow; the specimens reached 100 °C after about 10 min of cooling. After failure, which was considered to occur when more than 20 % of the top coat had spalled, the specimens were infiltrated in epoxy, cross-sectioned and polished for microscopy.

2.2. Interface roughness measurement

The interface roughness was measured on cross-sectioned specimens with an image analysis routine outlined in Fig. 2. The method involves the following steps: 1) Thresholding of the grayscale image to get a binary image, see Fig. 2 a) and b). 2) Acquisition of the interface roughness profile by simulating a profilometer stylus tip, see Fig. 2 c). 3) Filtering of the profile and establishing the mean line, see Fig. 2 d). 4) Cropping the profile to a suitable *sampling length*, see Fig. 2 e).

The results from image analysis were compared with results from a profilometer for some BC coated specimens (no top coat). This comparison was done to validate the accuracy of the image analysis derived surface roughness parameters, and to find a suitable magnification at which to perform the routine. Fig. 3 shows the results from this comparison; it can be seen that the results from the image analysis compares well to the results from the profilometer and that the lower magnification, with a resolution of 1.074 μm/pixel, was sufficient.

The setup used for image analysis can be summarised as: Roughness parameters were established and averaged from 65 interface roughness profiles with sampling lengths of 800 μm, thus resulting in a total examined length of about 5 cm which was considered enough to generate reliable mean values. The obtained profiles correspond to the BC/TGO interface. The simulated stylus tip had a radius of 5 μm. All wavelengths larger than the sampling length and smaller than two times the stylus tip radius were removed by Gaussian filtering.

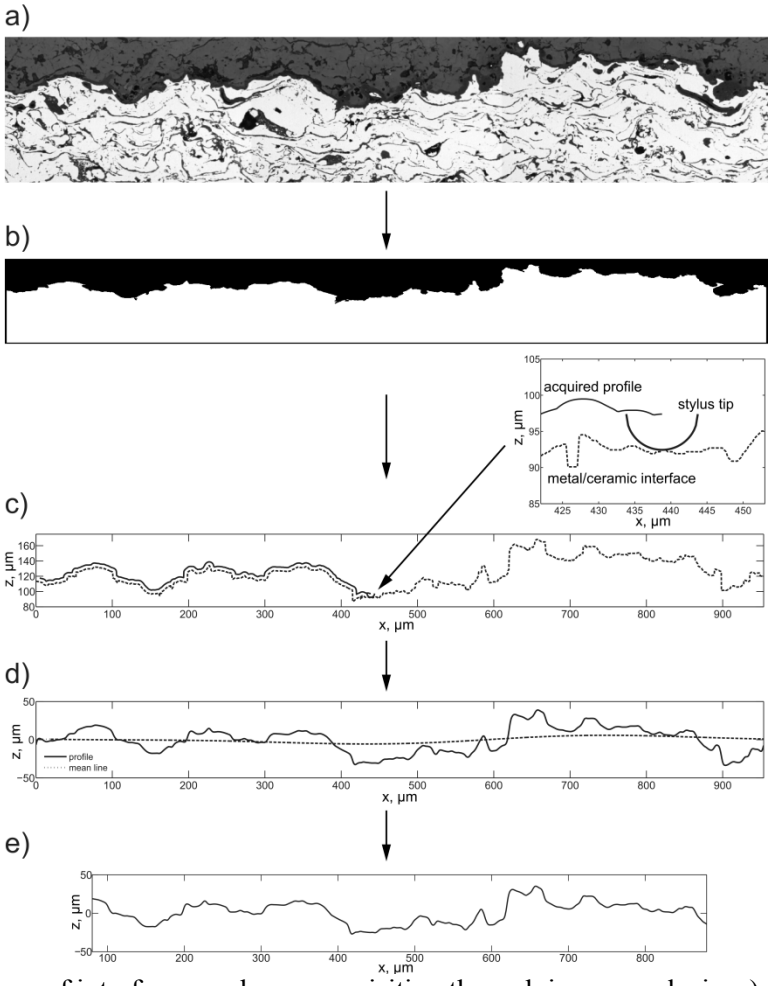

Figure 2. The process of interface roughness acquisition through image analysis: a) grayscale image b) binary image c) simulation of stylus tip d) filtering and mean line calculation e) final profile.

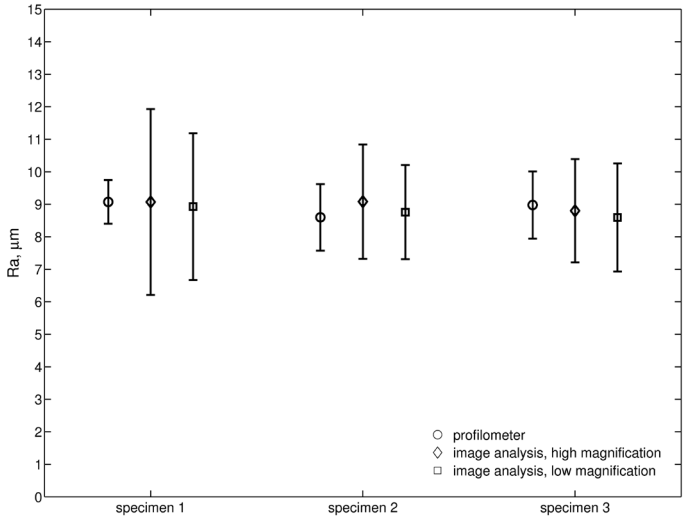

Figure 3. Comparison between the results from a profilometer and results obtained by image analysis performed on images with two different magnifications.

3. Results

3.1. Influence of interface roughness on the thermal fatigue life

The measured *Ra* and *Rc* of the specimens are presented in Fig. 4 as a function of the number of thermal cycles the specimens withstood until failure. There is a clear tendency for higher roughness (higher *Ra* and *Rc*) to give longer fatigue lives.

Fig. 5 shows the measured *RSm* and *RΔq* versus cycles to failure. *RSm* contains information about (wave)length, and *RΔq* contains information about both length and height. For *RΔq* a correlation with fatigue life exists where higher *RΔq* gives longer life. The same cannot be said for *RSm*, however, since the *RSm* value appears to be roughly equal for all specimens; the variation between the specimens is less than ± 5 % of the mean value of 232 µm.

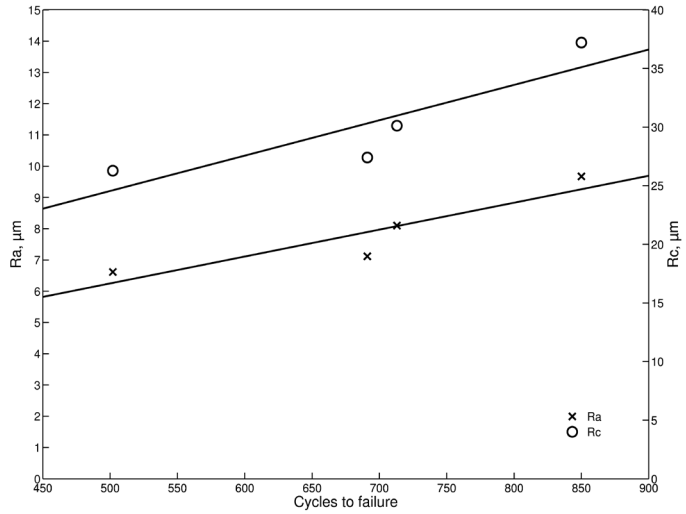

Figure 4. The influence of *Ra* and *Rc* on the thermal fatigue life.

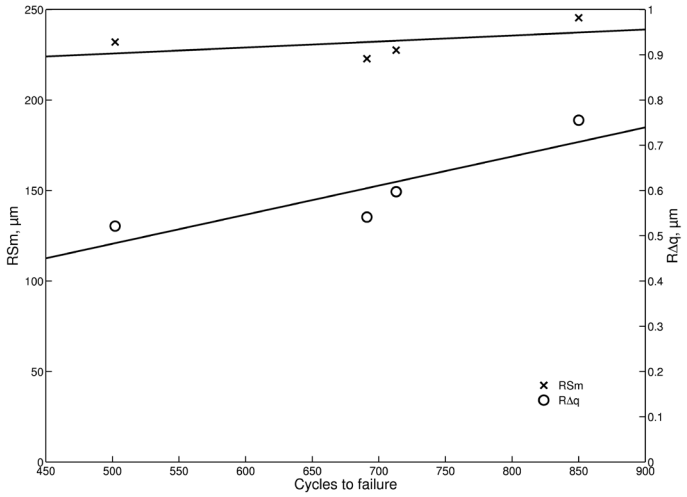

Figure 5. The influence of *RSm* and *RΔq* on the thermal fatigue life.

3.2. Interface models

In order to derive usable interface models, several assumptions have to be made. 1) Basing the model on measured interface roughness parameters will cause it to capture the main features of the actual interface. 2) Interface parameters that show a correlation with fatigue life (such as *Ra* and *Rc*) are appropriate to use as a base for model formulation. 3) For simplicity, the interface needs to be modelled as a periodic function.

Two models are presented here; they are both based on sine waves, see Eq. (5), as this is a commonly used shape for interface models in TBCs. The amplitude A and wavelength λ can then be derived from the interface roughness parameters as shown in Table 1.

$$z = A\sin\left(\frac{2\pi}{\lambda}x\right) \tag{5}$$

Model 1, see Table 1, is roughly the equivalence of measuring the height and wavelength directly in a micrograph. This model is based on *Rc* and *RSm* where *Rc* is twice the amplitude and *RSm* is the wavelength. Model 2 is derived from *Ra* and *RΔq*. It is obtained by entering Eq. (5) into Eq. (2) and its derivative into Eq. (4). Using the equations from Table 1 with Eq. (5) and values from Fig. 4 and 5, the amplitudes and wavelengths can be calculated and are listed in Table 2. For the remaining paper, only the specimen with lowest roughness (shortest life) and highest roughness (longest life) will be considered.

Table 1. Equations for the interface models.

Model	Amplitude	Wavelength
1	$A = Rc/2$	$\lambda = RSm$
2	$A = \frac{\pi Ra}{2}$	$\lambda = \frac{\pi\sqrt{2}}{R\Delta q}A$

Table 2. Amplitudes and wavelengths calculated from roughness parameters.

Specimen	Model	Amplitude, μm	Wavelength, μm
low roughness	1: *Rc*- and *RSm*-based	13.1	232
low roughness	2: *Ra*- and *RΔq*-based	10.4	89
high roughness	1: *Rc*- and *RSm*-based	18.6	245
high roughness	2: *Ra*- and *RΔq*-based	15.2	89

3.3. FE crack modelling

The two interface models were used for further FE modelling of crack growth under thermal stress. A fracture-mechanical analysis was done of a crack advancing along a sine-shaped interface of an idealised TBC. The analysis was done on a least representative cell of the TBC, as shown in Fig. 6 b), using the FE code Abaqus. The least representative cell was assumed to have a symmetry boundary on the left, and on the right hand boundary a kinematic boundary condition was applied causing the right boundary to remain plane. Crack growth was modelled both in the BC/TGO interface and the TGO/TC interface.

Fig. 6 shows the vertical stress component around a crack growing from a peak towards a valley in the TGO/TC interface. Fig. 7 shows the corresponding energy release rates, G, and stress intensity factors, K_I and K_{II}; the values in Fig. 7 are plotted versus *interface damage* where damage is defined as the horizontal length of the crack divided by half the wavelength, i.e. the damage is 1 when the crack reaches the valley. The K_I and K_{II} were obtained from Eq. (9) by post-processing of the results as demonstrated in the appendix. For both models, the specimen with high roughness gave higher G, K_I and K_{II} for most part of the crack growth; this was observed for both BC/TGO and TGO/TC cracks.

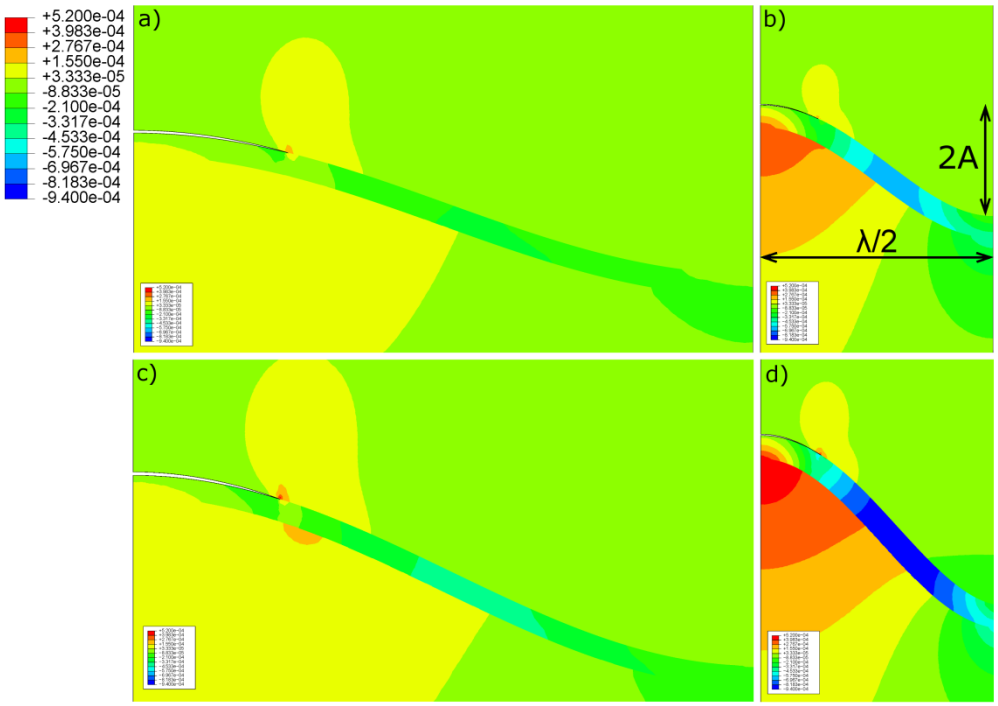

Figure 6. Vertical stress in the interface for: a) low roughness, model 1; b) low roughness, model 2; c) high roughness, model 1; d) high roughness, model 2.

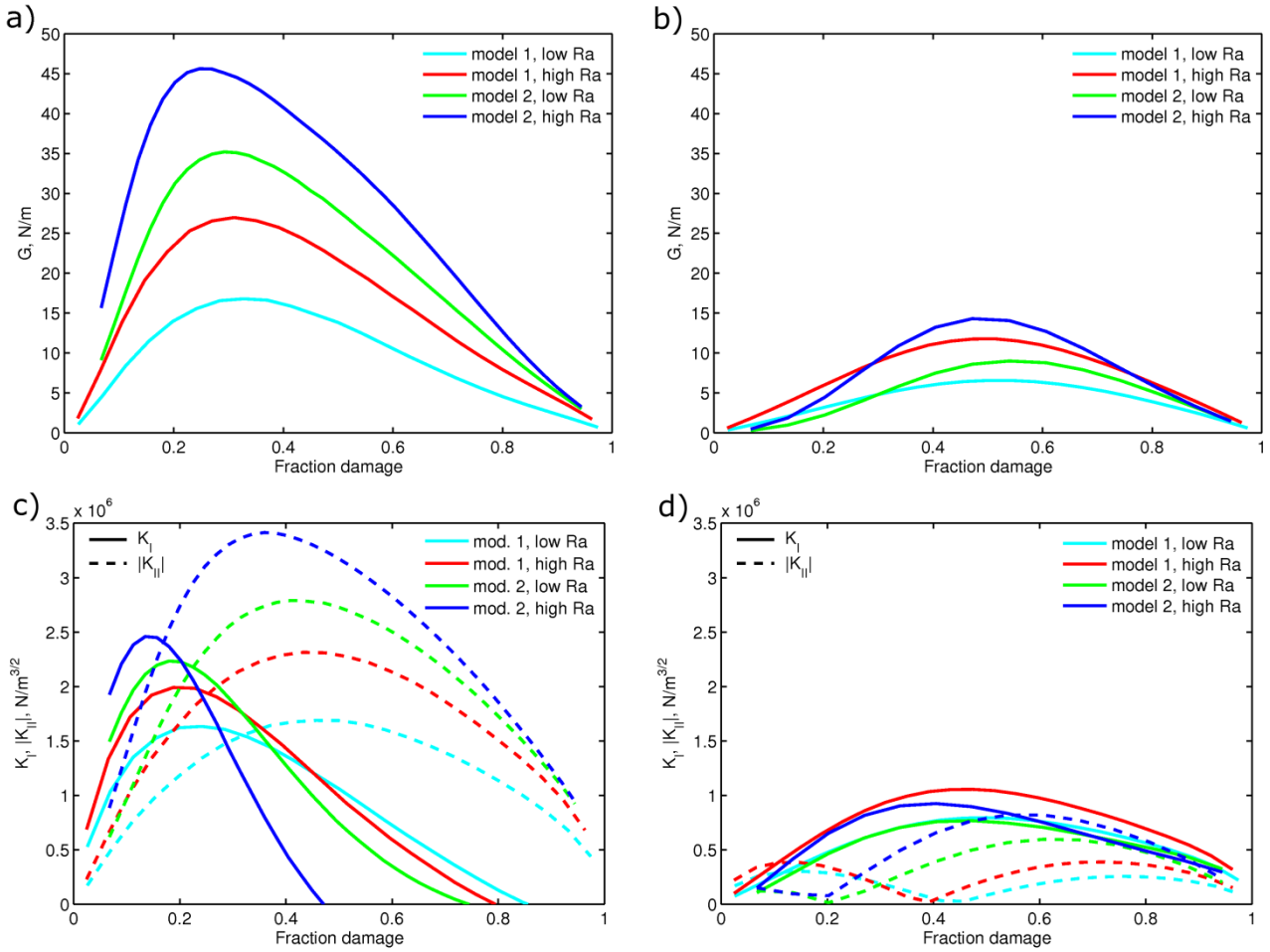

Figure 7. The calculated energy release rate, G, and stress intensity factors, K_I and K_{II} for a BC/TGO crack, a) and c), and a TGO/TC crack, b) and d).

4. Discussion

The large variation in fatigue life caused by different BC/TC interface roughness accentuates the importance of accurate interface models during FE modelling of crack growth in TBCs. Also other researchers have found the roughness to influence properties such as coating adhesion [8]. While earlier studies have investigated the influence of amplitude and wavelength on the stress field in TBCs by FE modelling [6,10-13], very little effort has been put on trying to derive those amplitudes and wavelengths from actual interfaces.

Both the suggested models were chosen so that they would agree well with the roughness parameters of the actual interfaces. Because of this, the models surely capture some of the characteristics of the interface. It is worth noting that the wavelength derived from $R\Delta q$ is the same for both specimens; also the *RSm* values indicate that the wavelengths of the specimens are in fact very similar. Casu et al. [9] argued that the wavelength could be correlated to the powder size during spraying; however, that is not the case for the specimens presented here.

The performed FE modelling may serve as a tool for evaluation of the relative behaviour of crack growth in the suggested interface models. Both model 1 and 2 showed an unexpected behaviour in that the G, as well as the K_I and K_{II}, increased with higher roughness; higher roughness was experimentally shown to increase fatigue life. Neither model 1 or 2 thus capture the experimentally observed tendency for higher interface roughness to promote longer fatigue lives.

Several explanations for this discrepancy exist, among them:

- The sine wave may be an inappropriate shape for modelling the interface.
- The increase in mechanical adhesion caused by the rougher interface may outweigh the detrimental effects of higher stresses in the interface.
- Cracks may grow in different ways than modelled here.

It is evident that further work remains before an FE model can accurately capture the experimentally observed tendency for higher interface roughness to promote longer fatigue life.

5. Conclusions

The bond coat/top coat interface roughness was shown to largely influence the thermal fatigue life of TBCs where higher roughness gave longer lives. Various roughness parameters were calculated from the interface roughness profiles, which were obtained by image analysis. *Ra*, *Rc* and *RΔq* were found to have a correlation with fatigue life where higher values gave longer life. The spacing parameter *RSm* was essentially the same for all specimens and could not have had an effect on the fatigue life. These parameters were used to establish two sine shaped interface models which were applied to FE modelling of crack growth in the specimens with shortest and longest life. The K_I and K_{II} were compared for the two specimens. Neither of the suggested models appeared to capture the experimentally observed tendency for increased life with higher roughness; the K_I and K_{II} increased with higher roughness for both suggested models. This study resulted in two interface models which were directly derived from the actual interface, but also showed that much work remains before accurate interface models can be formulated.

Acknowledgements

This research has been funded by the Swedish Energy Agency, Siemens Industrial Turbomachinery AB, GKN Aerospace Engine Systems, and the Royal Institute of Technology, through the Swedish research programme TURBO POWER, the support of which is gratefully acknowledged.

References

[1] J.T. DeMasi-Marcin, D.K. Gupta, Protective Coatings in the Gas Turbine Engine, Surf. Coat. Technol. 68/69 (1994) 1–9.

[2] H.E. Evans, M.P. Taylor, Oxidation of high-temperature coatings, Proc. IMechE, J. Aerospace Engineering. 220 (2006) 1–10.

[3] G.W. Goward, Progress in coatings for gas turbine airfoils, Surf. Coat. Technol. 108/109 (1998) 73–79.

[4] M.J. Pomeroy, Coatings for gas turbine materials and long term stability issues, Mater. Des. 26 (2005) 223–231.

[5] S. Sjostrom, H. Brodin, Thermomechanical fatigue life of TBCs - experimental and modelling aspects, Ceram. Eng. Sci. Proc. 31 (2010) 23–39.

[6] M. Jinnestrand, S. Sjostrom, Investigation of 3D FE simulations of delamination crack initiation in TBC caused by alumina growth, Surf. Coat. Technol. 135 (2001) 188–195.

[7] H. Brodin, R. Eriksson, S. Johansson, S. Sjostrom, Fracture mechanical modelling of a plasma sprayed TBC system, Ceram. Eng. Sci. Proc. 30 (2010) 113–124.

[8] A. Nusair Khan, J. Lu, H. Liao, Effect of residual stresses on air plasma sprayed thermal barrier coatings, Surf. Coat. Technol. 168 (2003) 291–299.

[9] A. Casu, J. Marques, R. Valien, D. Stover, Numerical simulation of crack growth mechanisms occurring near the bondcoat surface in air plasma sprayed thermal barrier coatings, Ceram. Eng. Sci. Proc. 27 (2007) 115–126.

[10] M. Ahrens, R. Vafien, D. Stover, Stress distributions in plasma-sprayed thermal barrier coatings as a function of interface roughness and oxide scale thickness, Surf. Coat. Technol. 161 (2002) 26–35.

[11] M. Baker, J. Rosler, G. Heinze, A parametric study of the stress state of thermal barrier coatings, Acta Mater. 53 (2005) 469–476.

[12] Y. Liu, C. Persson, J. Wigren, Experimental and Numerical Life Prediction of Thermally Cycled Thermal Barrier Coatings, J. Therm. Spray Technol. 13 (2004) 415–424.

[13] J. Aktaa, K. Sfar, D. Munz, Assessment of TBC systems failure mechanisms using a fracture mechanics approach, Acta Mater. 53 (2005) 4399–4413.

[14] E.S. Gadelmawla, M.M. Koura, T.M.A. Maksoud, I.M. Elewa, H.H. Soliman, Roughness parameters, J. Mater. Process. Technol. 123 (2002) 133–145.

[15] J.W. Hutchinson, Z. Suo, Mixed Mode Cracking in Layered Materials, Advances in Applied Mechanics. 29 (1991) 63–191.

Appendix: Mechanics of the interface crack

From the FE solution, the energy release rate G and the crack flank displacements $u_1^{(u)}$, $u_1^{(l)}$, $u_2^{(u)}$ and $u_2^{(l)}$ at a number of nodes along the crack flank are used.

For a description of the theory of an interface crack see, for instance, [15].
The relation between G, K_I and K_{II} is given by

$$G = \frac{1}{H}(K_I^2 + K_{II}^2) \tag{6}$$

in which

$$H = \frac{2\cosh^2(\pi\epsilon)}{\frac{1}{E_1^*} + \frac{1}{E_2^*}}$$

$$\epsilon = \frac{1}{2\pi}\ln\frac{\frac{1+\nu_2}{E_2}+\kappa_1\frac{1+\nu_1}{E_1}}{\kappa_2\frac{1+\nu_2}{E_2}+\frac{1+\nu_1}{E_1}}$$

$$\kappa_i = \begin{cases} 3-4\nu_i \text{ ; plane strain} \\ \dfrac{3-\nu_i}{1+\nu_i} \text{ ; plane stress} \end{cases} ; i = 1,2$$

$$E_i^* = \begin{cases} \dfrac{E_i}{1-\nu_i^2} \text{ ; plane strain} \\ E_i \text{ ; plane stress} \end{cases} ; i = 1,2$$

Using the general fracture-mechanical solution for an interface crack, $\delta_1 = u_1^{(u)} - u_1^{(l)}$ and $\delta_2 = u_2^{(u)} - u_2^{(l)}$ are then given by

$$\begin{bmatrix}\delta_1 \\ \delta_2\end{bmatrix} = \Psi \cdot \begin{bmatrix}\sin(\epsilon\ln r) - 2\epsilon\cos(\epsilon\ln r) & 2\epsilon\sin(\epsilon\ln r) + \cos(\epsilon\ln r) \\ 2\epsilon\sin(\epsilon\ln r) + \cos(\epsilon\ln r) & -\sin(\epsilon\ln r) + 2\epsilon\cos(\epsilon\ln r)\end{bmatrix}\begin{bmatrix}K_I \\ K_{II}\end{bmatrix} \tag{7}$$

where

$$\Psi = \frac{1}{2}\left(\frac{1}{E_1^*}+\frac{1}{E_2^*}\right)\cdot\frac{8}{(1+4\epsilon^2)\cosh(\pi\epsilon)}\cdot\left(\frac{r}{2\pi}\right)^{\frac{1}{2}}$$

Eq. (7) is only used for establishing an expression for $\beta = K_I/K_{II}$:

$$\beta = \frac{K_I}{K_{II}} = \frac{[\sin(\epsilon\ln r) - 2\epsilon\cos(\epsilon\ln r)]\cdot\delta_1 + [2\epsilon\sin(\epsilon\ln r) + \cos(\epsilon\ln r)]\cdot\delta_2}{[2\epsilon\sin(\epsilon\ln r) + \cos(\epsilon\ln r)]\cdot\delta_1 - [\sin(\epsilon\ln r) - 2\epsilon\cos(\epsilon\ln r)]\cdot\delta_2} \tag{8}$$

By combining Eq. (6) and (8) we finally get

$$\begin{cases} K_I = \sqrt{\dfrac{GH}{1+\dfrac{1}{\beta^2}}} \\ K_{II} = \sqrt{\dfrac{GH}{1+\beta^2}} \end{cases} \tag{9}$$